

## Supporting information

### Studying the mechanism of phase separation in aqueous solutions of globular proteins via molecular dynamics computer simulations

Sandi Brudar, Jure Gujt, Eckhard Spohr, and Barbara Hribar-Lee\*

E-mail: [barbara.hribar@fkkt.uni-lj.si](mailto:barbara.hribar@fkkt.uni-lj.si)

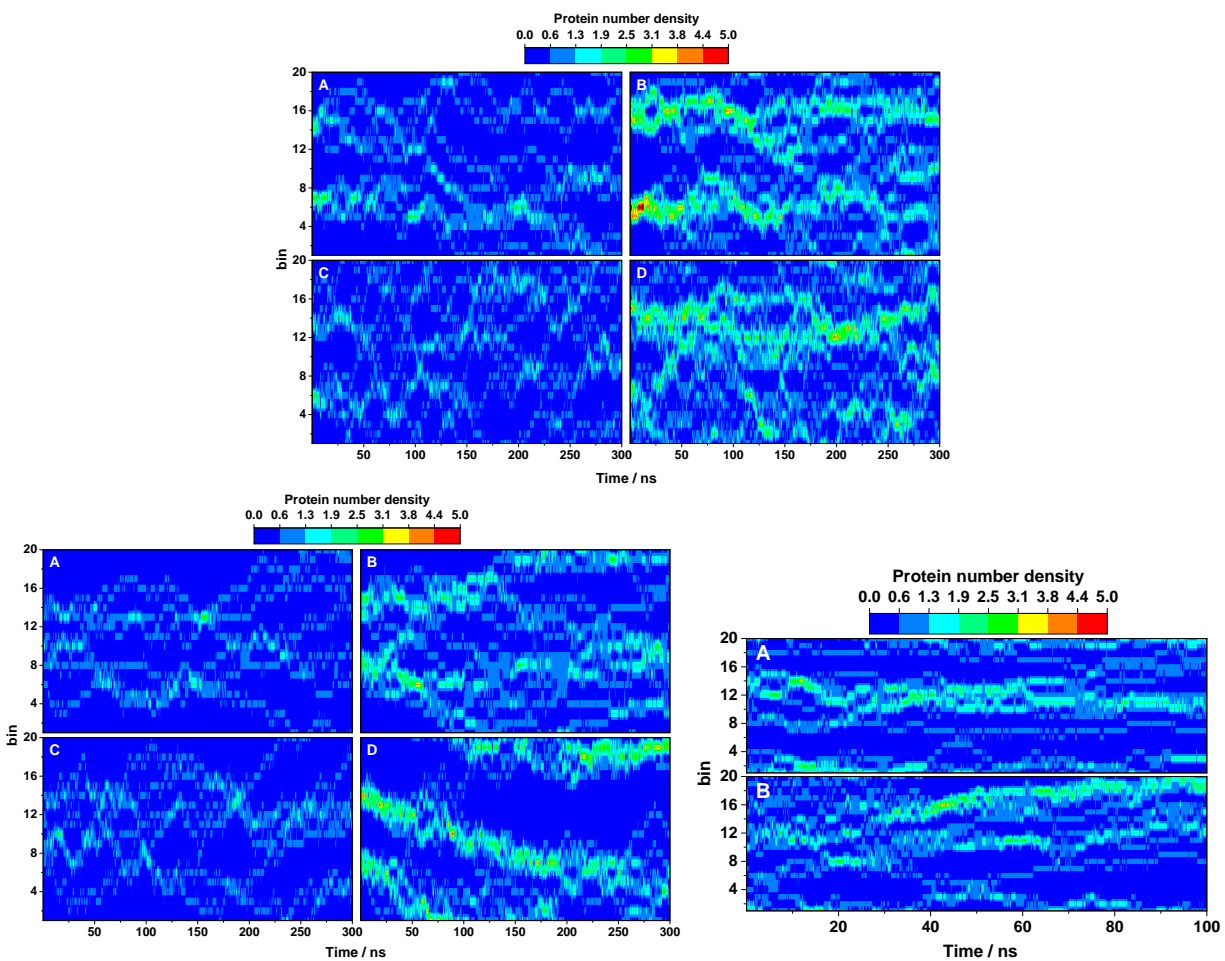


Figure S1: Density fluctuations of proteins in the y-axis direction. HEWL (top line) at 42 mg/mL (A at 267 K, C at 300 K) and 93 mg/mL (B at 267 K and D at 300 K). T4 WT\* (bottom left) at 45 mg/mL (A at 267 K and C at 300 K) and 90 mg/mL (B at 267 K and D at 300 K).  $\gamma$ -D crystallin (bottom right) at 100 mg/mL (A at 300 K and B at 320 K).

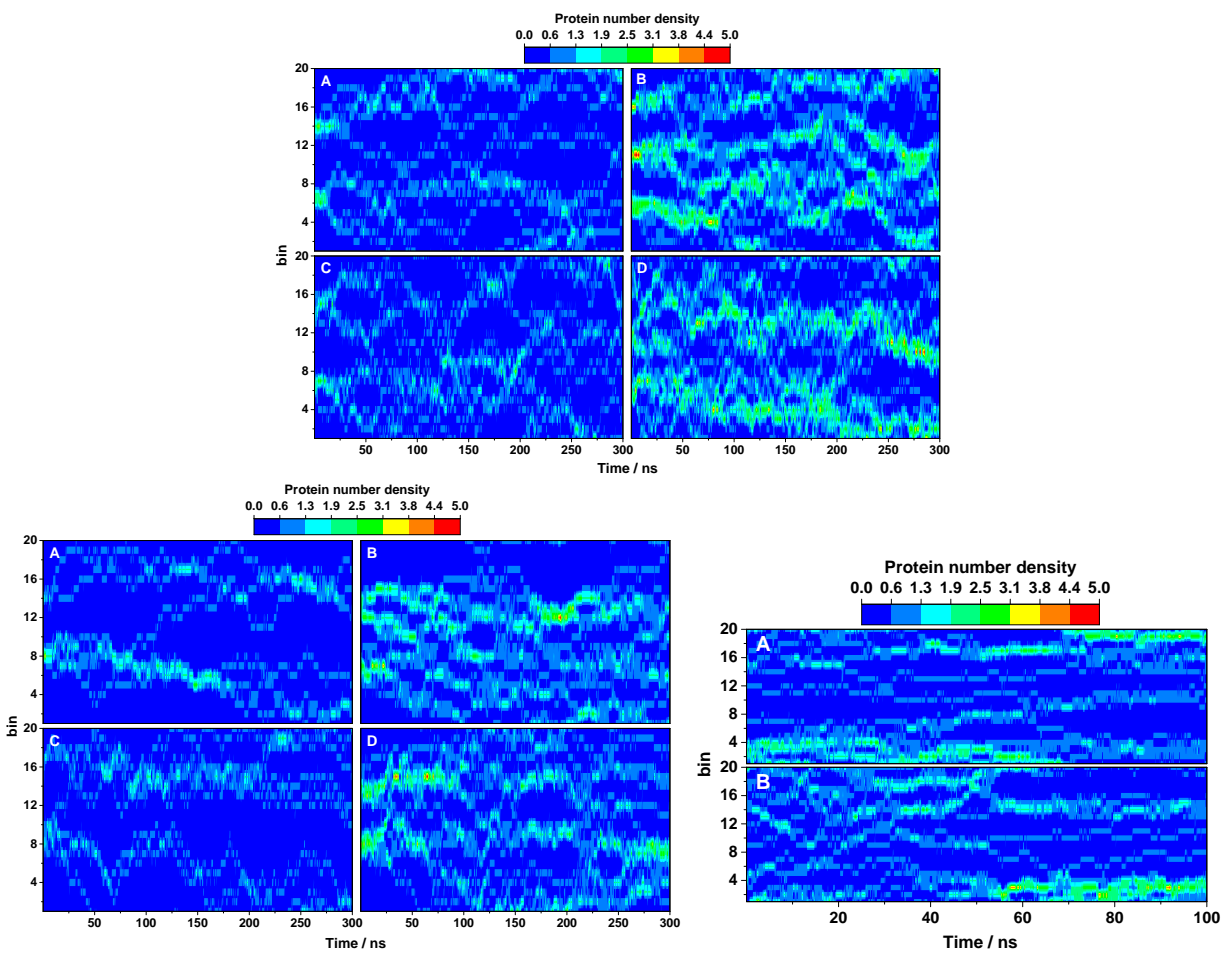


Figure S2: Density fluctuations of proteins in the z-axis direction. HEWL (top line) at 42 mg/mL (A at 267 K, C at 300 K) and 93 mg/mL (B at 267 K and D at 300 K). T4 WT\* (bottom left) at 45 mg/mL (A at 267 K and C at 300 K) and 90 mg/mL (B at 267 K and D at 300 K).  $\gamma$ -D crystallin (bottom right) at 100 mg/mL (A at 300 K and B at 320 K).

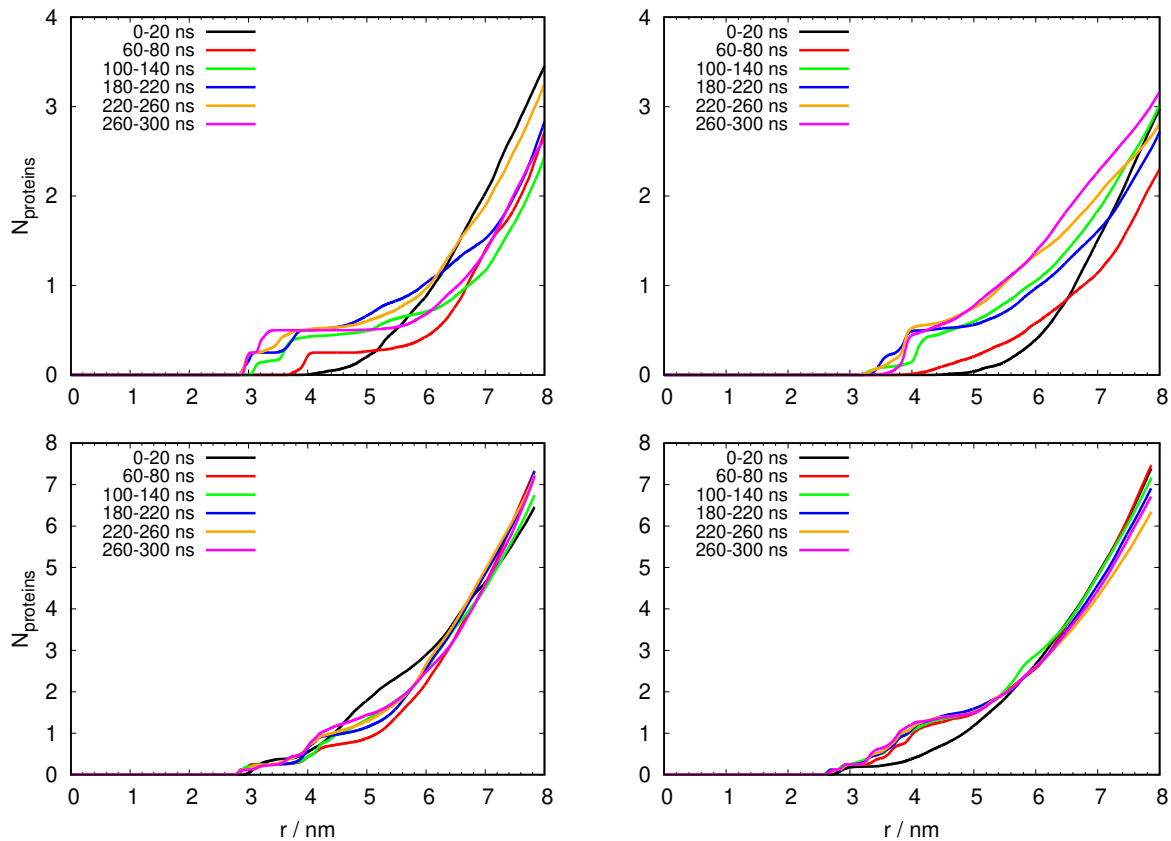


Figure S3: The number of protein molecules at different times of the simulation in the vicinity of HEWL molecule at 42 mg/mL (top left 267 K and top right 300 K) and 93 mg/mL (bottom left 267 K and bottom right 300 K)

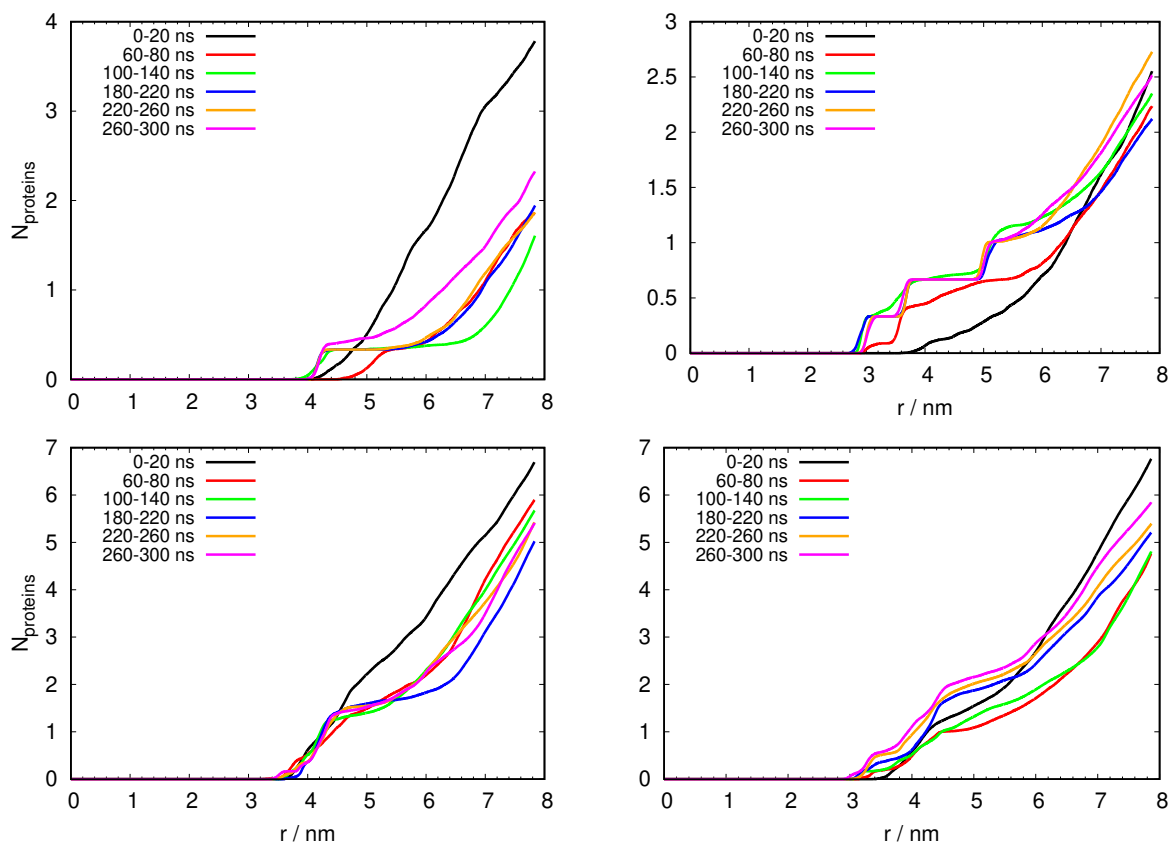


Figure S4: The number of protein molecules at different times of the simulation in the vicinity of T4 WT\* molecule at 45 mg/mL (top left 267 K and top right 300 K) and 90 mg/mL (bottom left 267 K and bottom right 300 K).

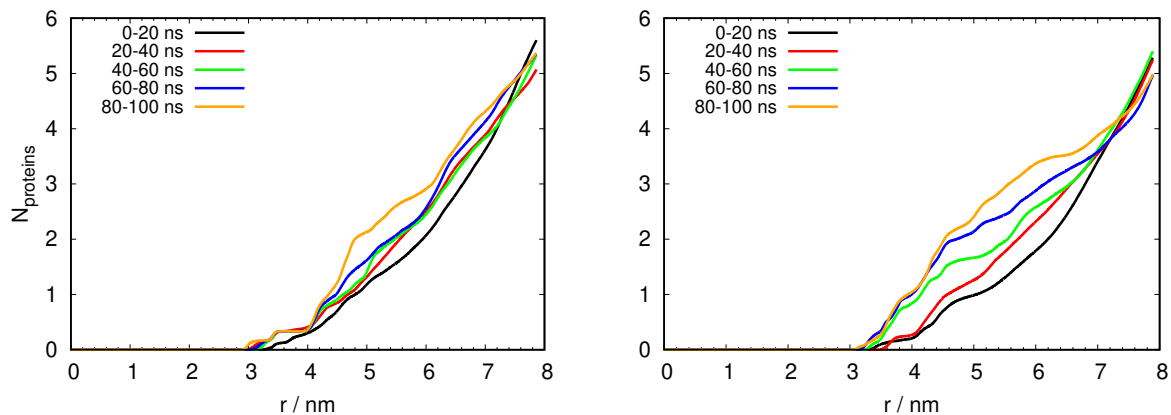


Figure S5: The number of protein molecules at different times of the simulation in the vicinity of  $\gamma$ -D crystallin molecule at 100 mg/mL (left 300 K and right 320 K).

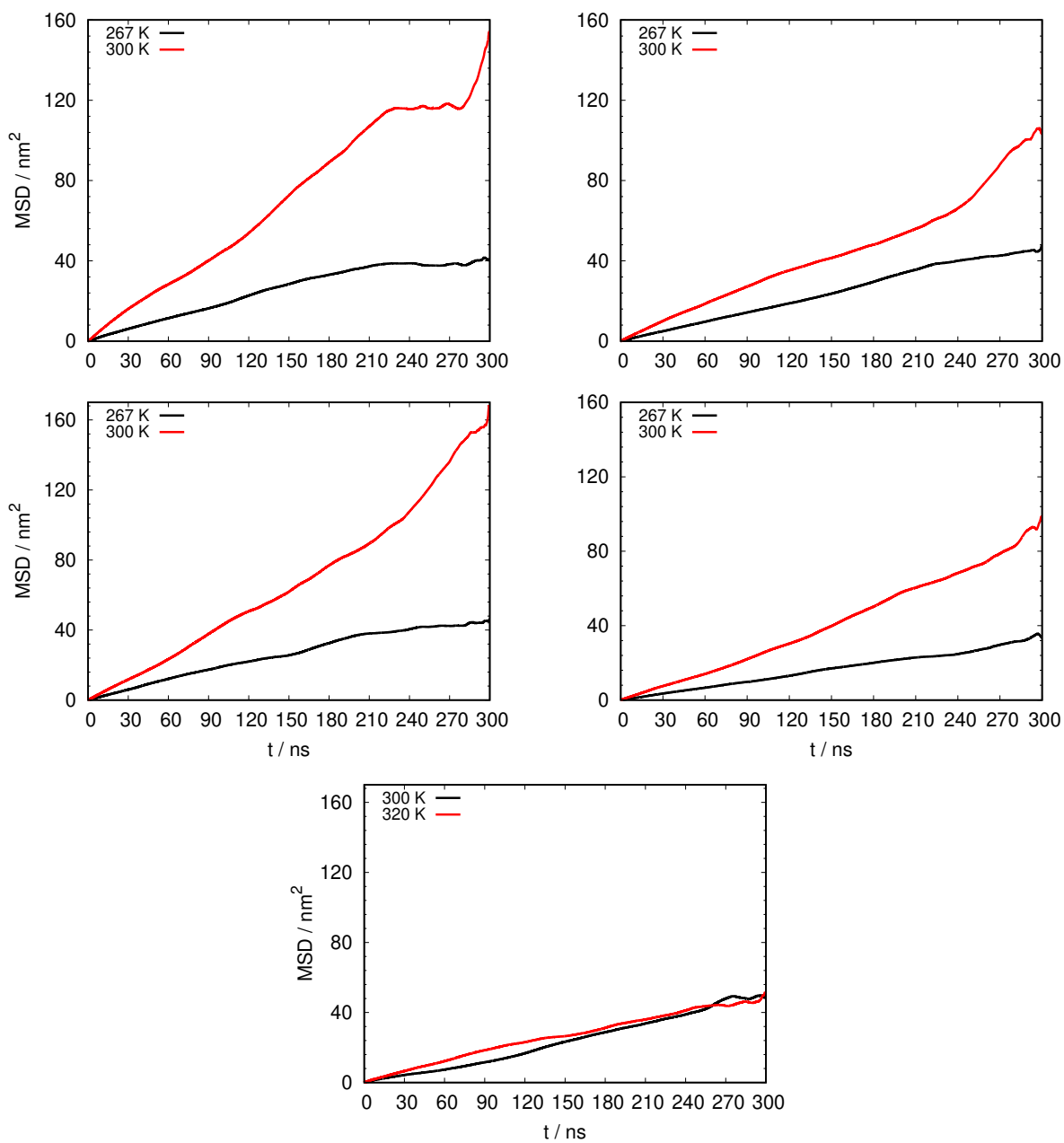


Figure S6: Mean square displacement of proteins at different temperatures. HEWL at 42 mg/mL (top left) and 93 mg/mL (top right). T4 WT\* at 45 mg/mL (middle left) and at 90 mg/mL (middle right).  $\gamma$ -D crystallin at 100 mg/mL (bottom).

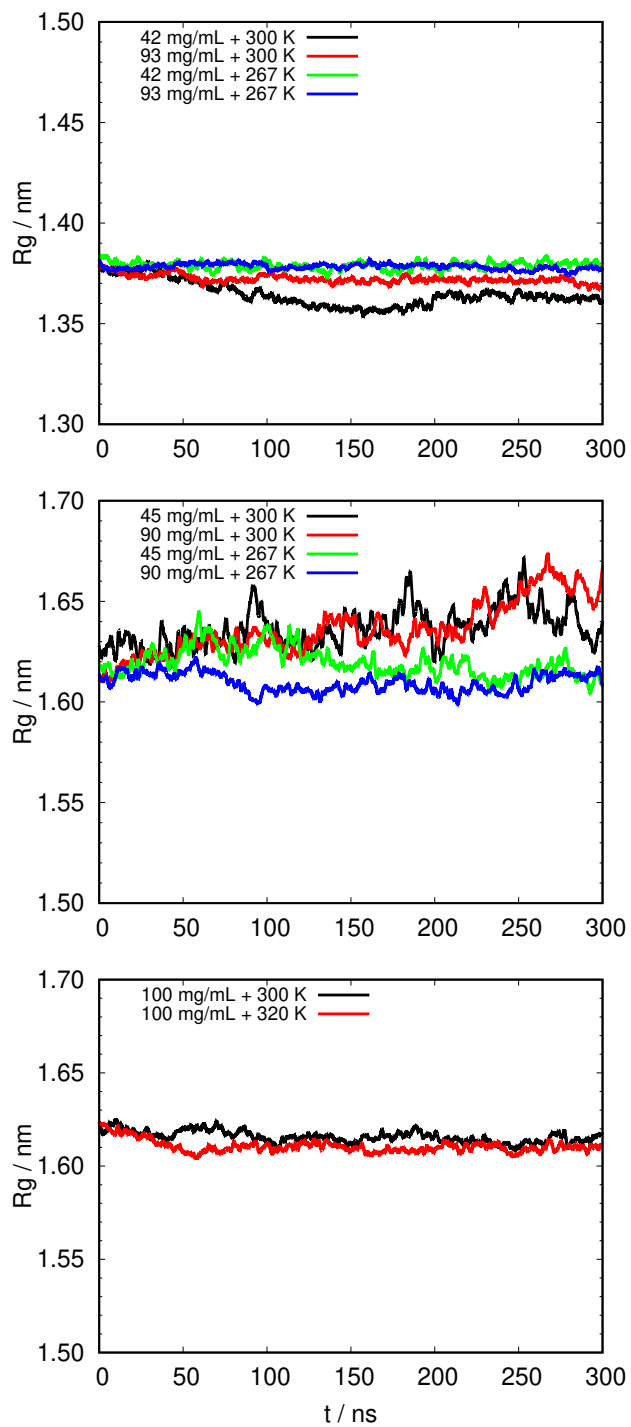


Figure S7: The radius of gyration of HEWL (top), T4 WT\* lysozyme (middle) and of  $\gamma$ -D crystallin (bottom).

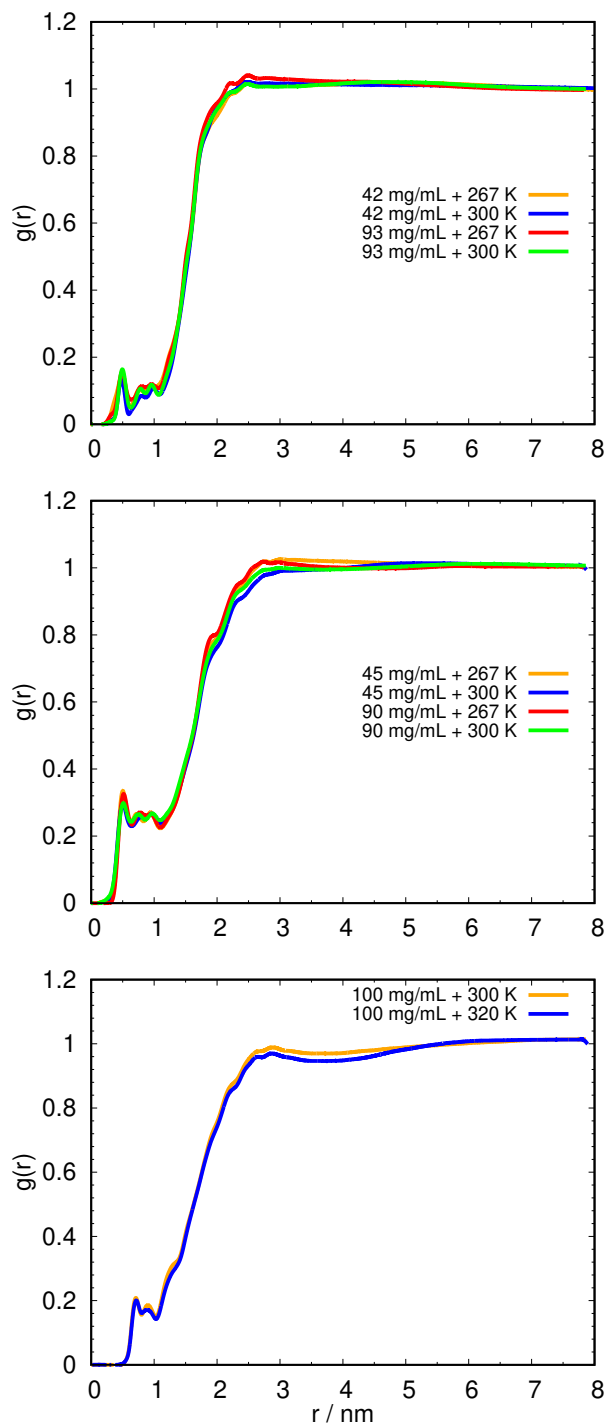


Figure S8: The water oxygen - protein center of mass pair distribution functions for HEWL (top), T4 WT\* lysozyme (middle) and  $\gamma$ -D crystallin (bottom).

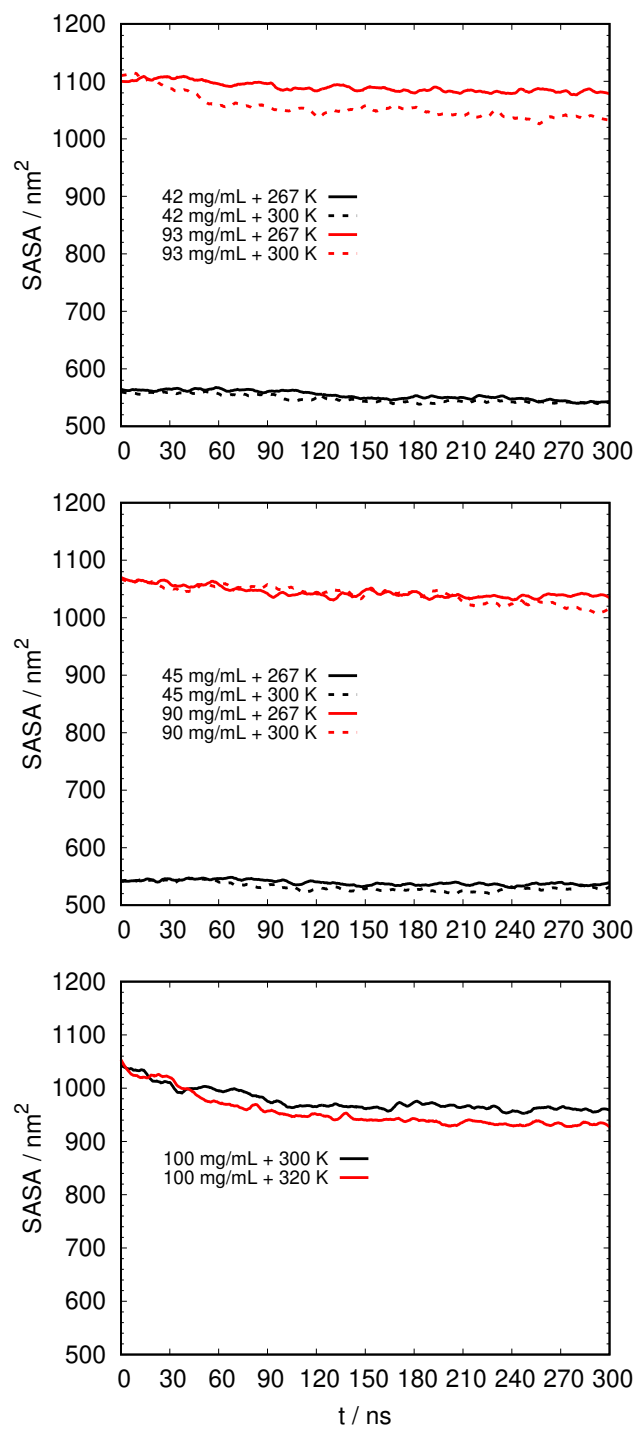


Figure S9: Solvent accessible surface area (SASA) for HEWL (top), T4 WT\* lysozyme (middle) and  $\gamma$ -D crystallin (bottom).

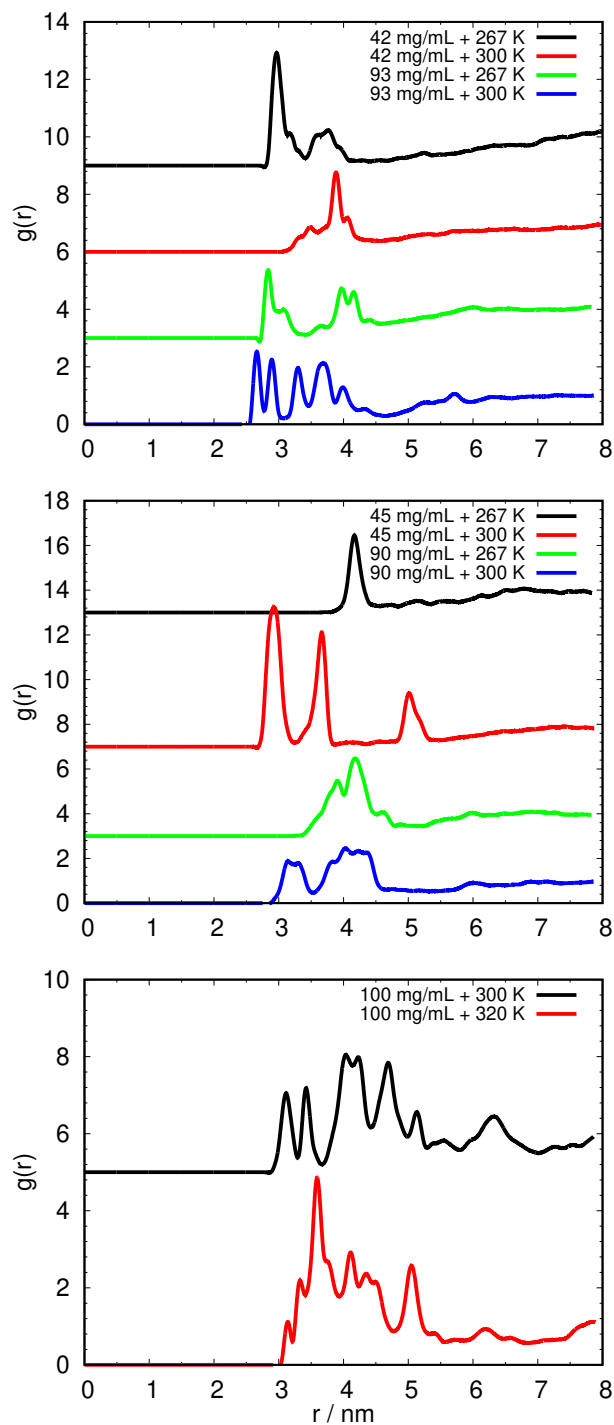


Figure S10: Protein-protein pair distribution functions for HEWL (top), T4 WT\* lysozyme (middle) and  $\gamma$ -D crystallin (bottom). Plots are shifted vertically for clarity.

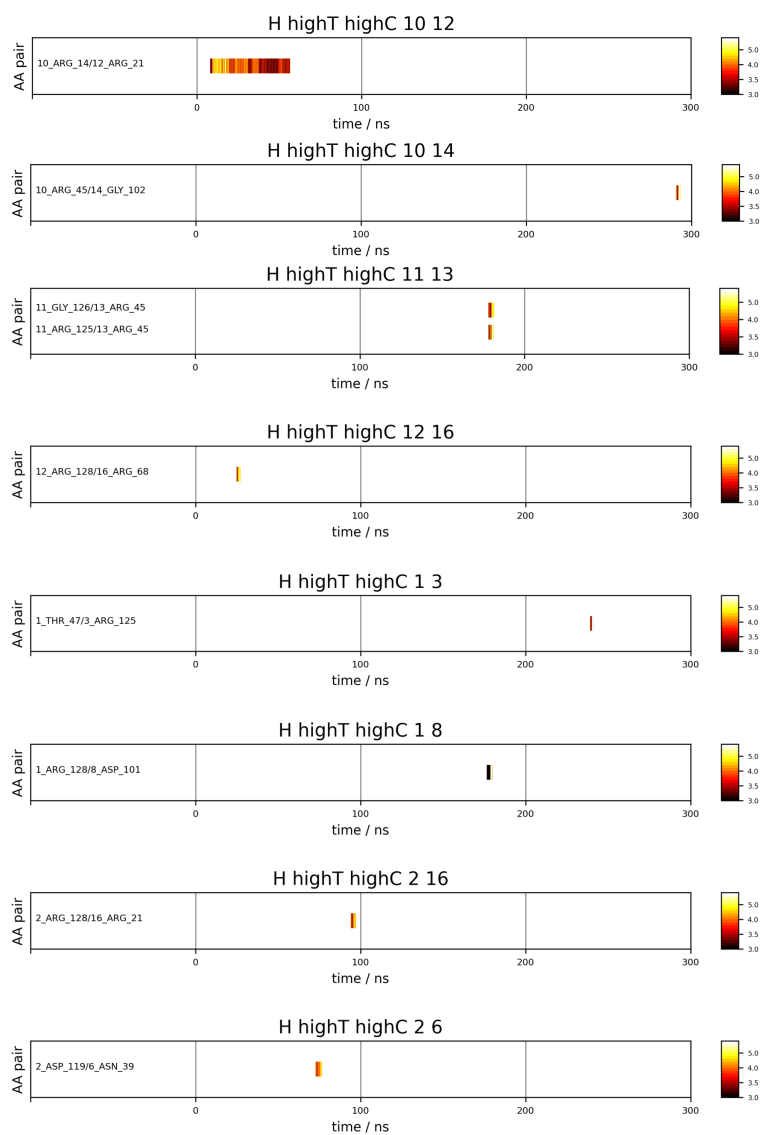


Figure S11: Time evolution of residue-residue contacts that appear within 6 Å between different pairs of HEWL molecules in the solution comprising of 93 mg mL<sup>-1</sup> of HEWL at 300 K. The shortest distance (here in Å) between the residue pairs is represented with a heat map on the right. Distances above 6 Å are plotted as white space

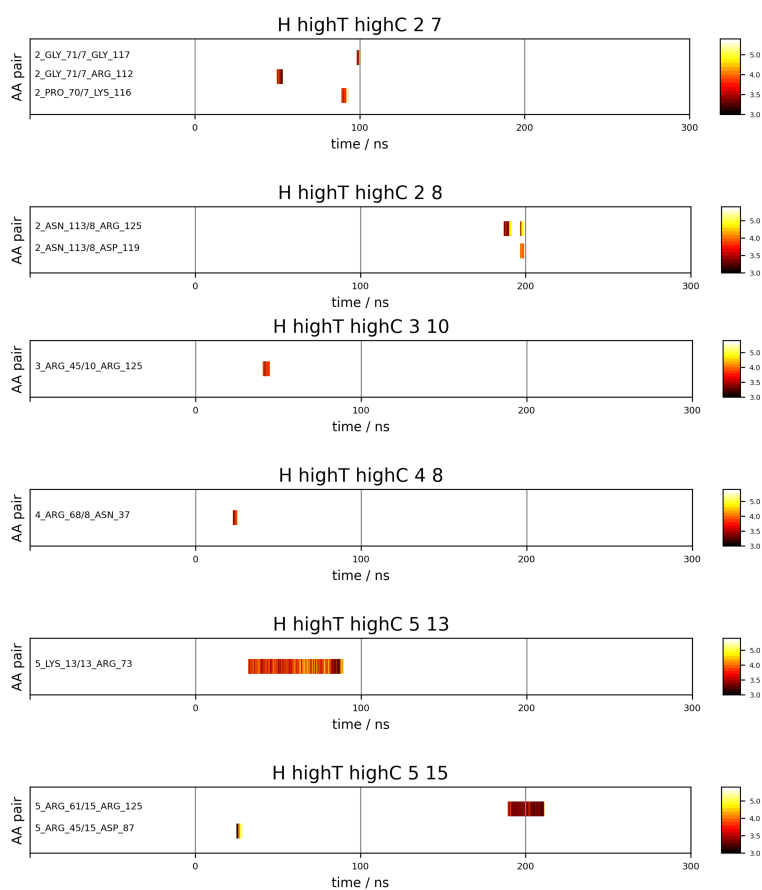


Figure S12: Time evolution of residue-residue contacts that appear within  $6 \text{ \AA}$  between different pairs of HEWL molecules in the solution comprising of  $93 \text{ mg mL}^{-1}$  of HEWL at 300 K. The shortest distance (here in  $\text{\AA}$ ) between the residue pairs is represented with a heat map on the right. Distances above  $6 \text{ \AA}$  are plotted as white space.

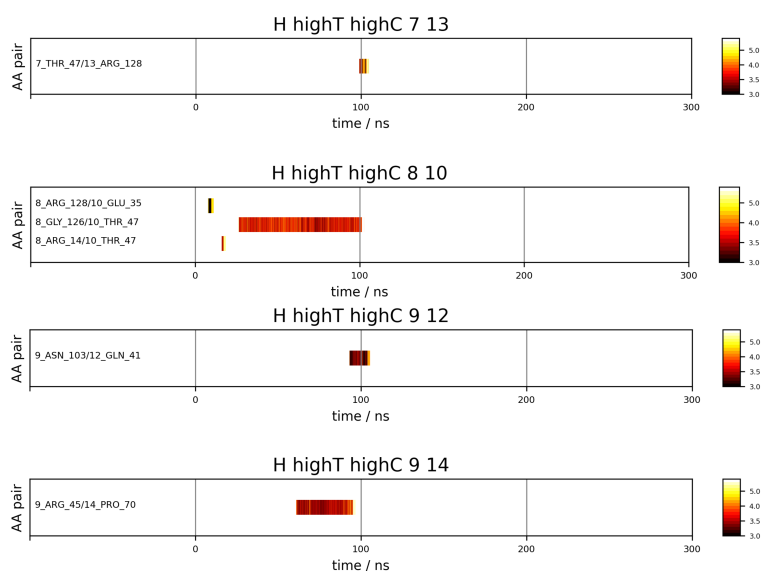


Figure S13: Time evolution of residue-residue contacts that appear within 6 Å between different pairs of HEWL molecules in the solution comprising of 93 mg mL<sup>-1</sup> of HEWL at 300 K. The shortest distance (here in Å) between the residue pairs is represented with a heat map on the right. Distances above 6 Å are plotted as white space.

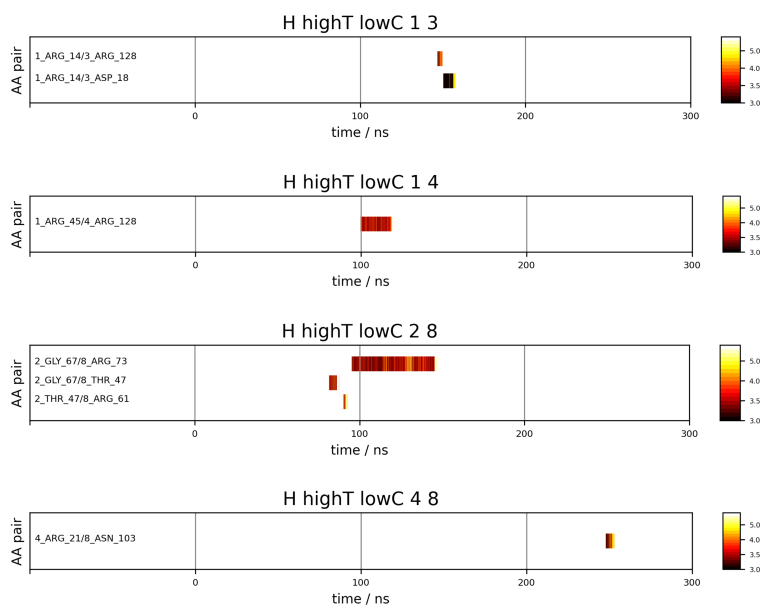


Figure S14: Time evolution of residue-residue contacts that appear within 6 Å between different pairs of HEWL molecules in the solution comprising of 42 mg mL<sup>-1</sup> of HEWL at 300 K. The shortest distance (here in Å) between the residue pairs is represented with a heat map on the right. Distances above 6 Å are plotted as white space.

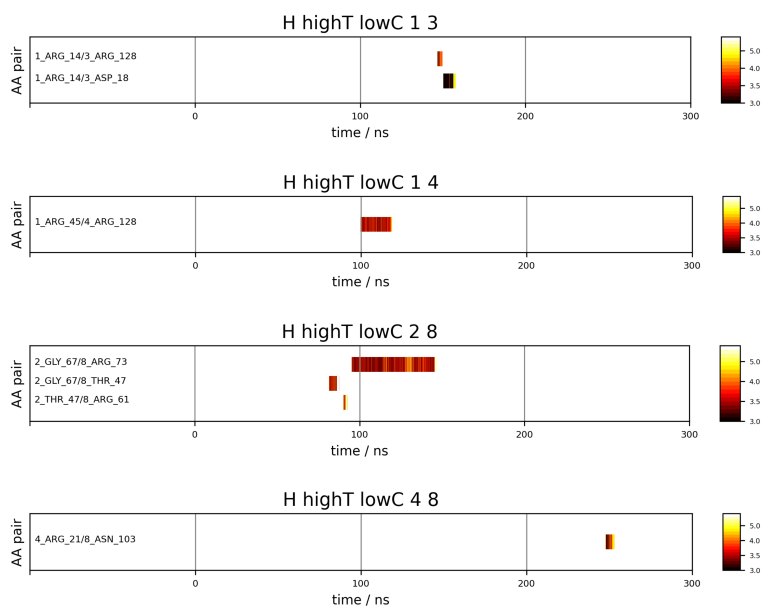


Figure S15: Time evolution of residue-residue contacts that appear within 6 Å between different pairs of HEWL molecules in the solution comprising of 42 mg mL<sup>-1</sup> of HEWL at 300 K. The shortest distance (here in Å) between the residue pairs is represented with a heat map on the right. Distances above 6 Å are plotted as white space.

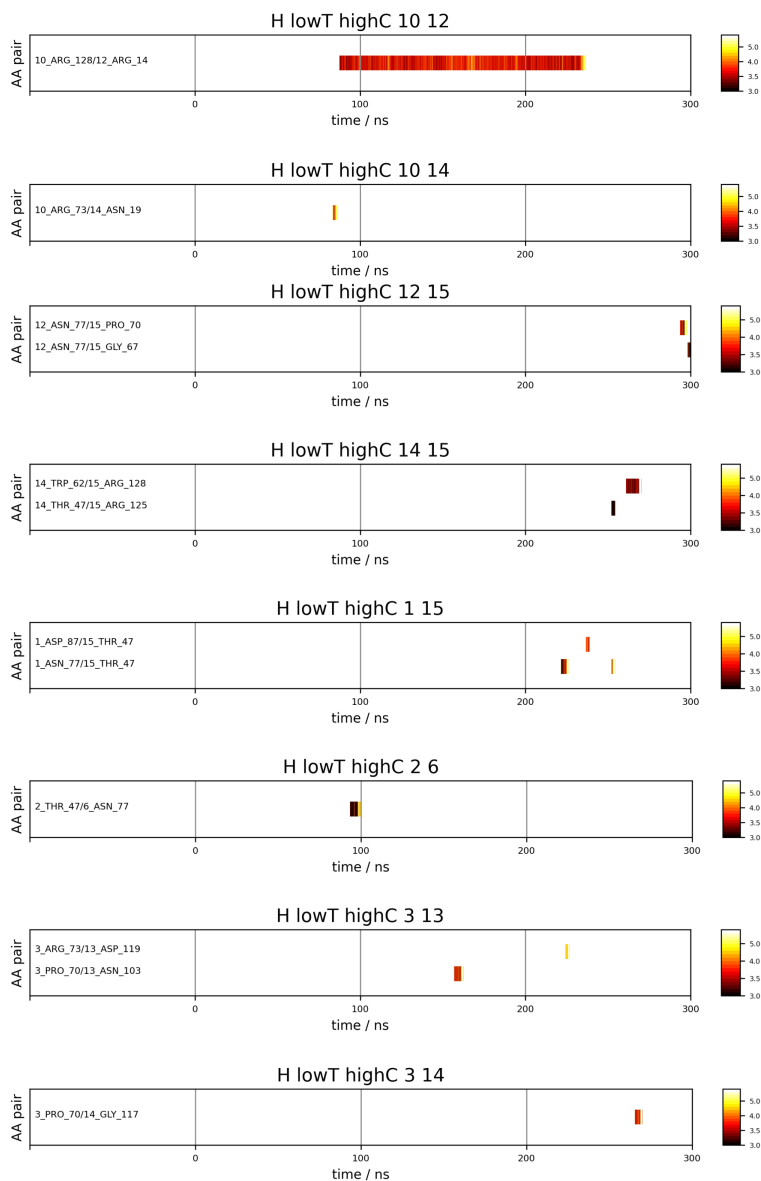


Figure S16: Time evolution of residue-residue contacts that appear within 6 Å between different pairs of HEWL molecules in the solution comprising of 93 mg mL<sup>-1</sup> of HEWL at 267 K. The shortest distance (here in Å) between the residue pairs is represented with a heat map on the right. Distances above 6 Å are plotted as white space.

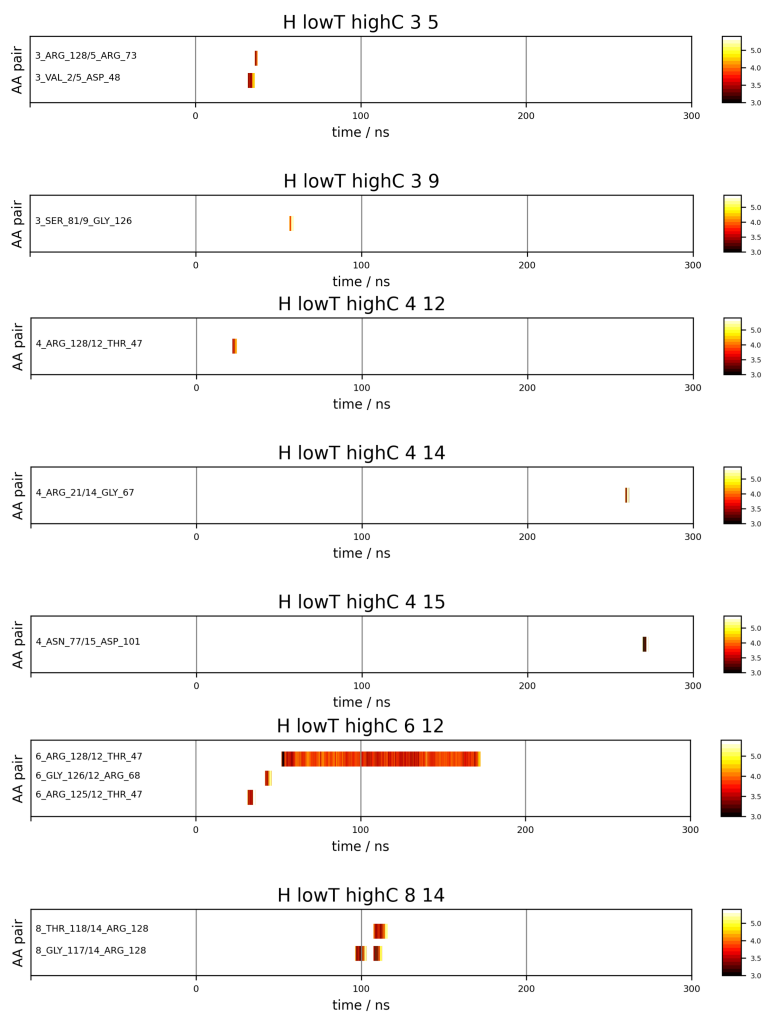


Figure S17: Time evolution of residue-residue contacts that appear within  $6 \text{ \AA}$  between different pairs of HEWL molecules in the solution comprising of  $93 \text{ mg mL}^{-1}$  of HEWL at  $267 \text{ K}$ . The shortest distance (here in  $\text{\AA}$ ) between the residue pairs is represented with a heat map on the right. Distances above  $6 \text{ \AA}$  are plotted as white space.

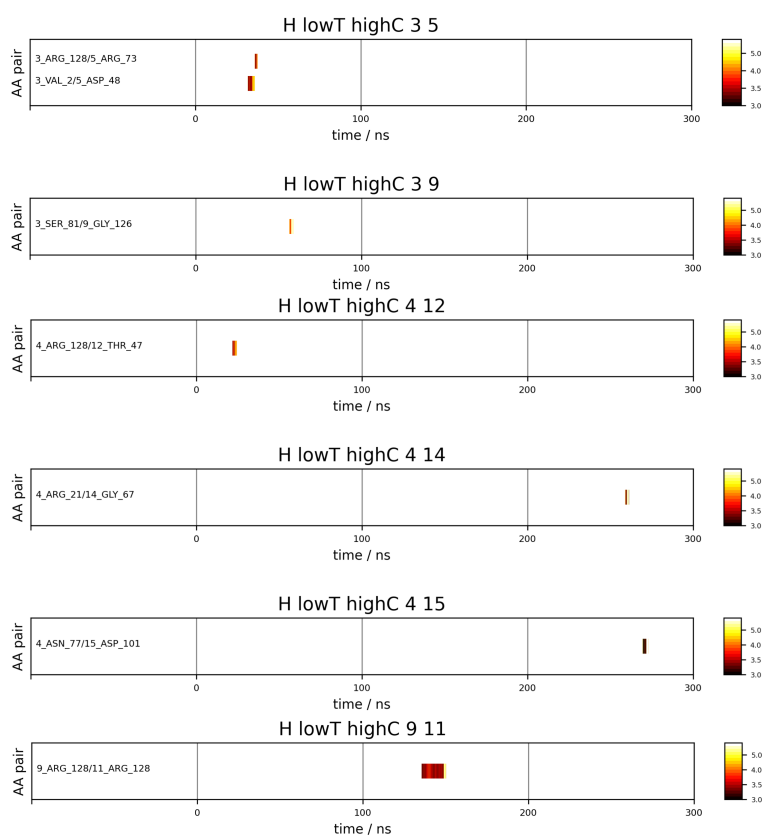


Figure S18: Time evolution of residue-residue contacts that appear within  $6 \text{ \AA}$  between different pairs of HEWL molecules in the solution comprising of  $93 \text{ mg mL}^{-1}$  of HEWL at 267 K. The shortest distance (here in  $\text{\AA}$ ) between the residue pairs is represented with a heat map on the right. Distances above  $6 \text{ \AA}$  are plotted as white space.

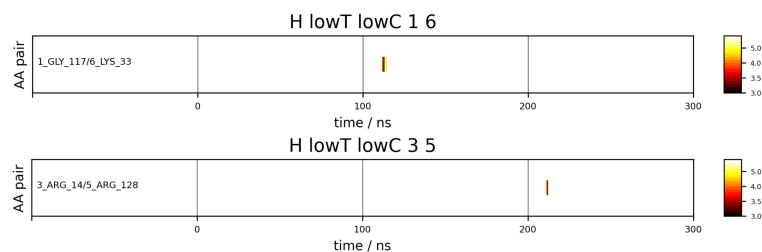


Figure S19: Time evolution of residue-residue contacts that appear within  $6 \text{ \AA}$  between different pairs of HEWL molecules in the solution comprising of  $42 \text{ mg mL}^{-1}$  of HEWL at 267 K. The shortest distance (here in  $\text{\AA}$ ) between the residue pairs is represented with a heat map on the right. Distances above  $6 \text{ \AA}$  are plotted as white space.

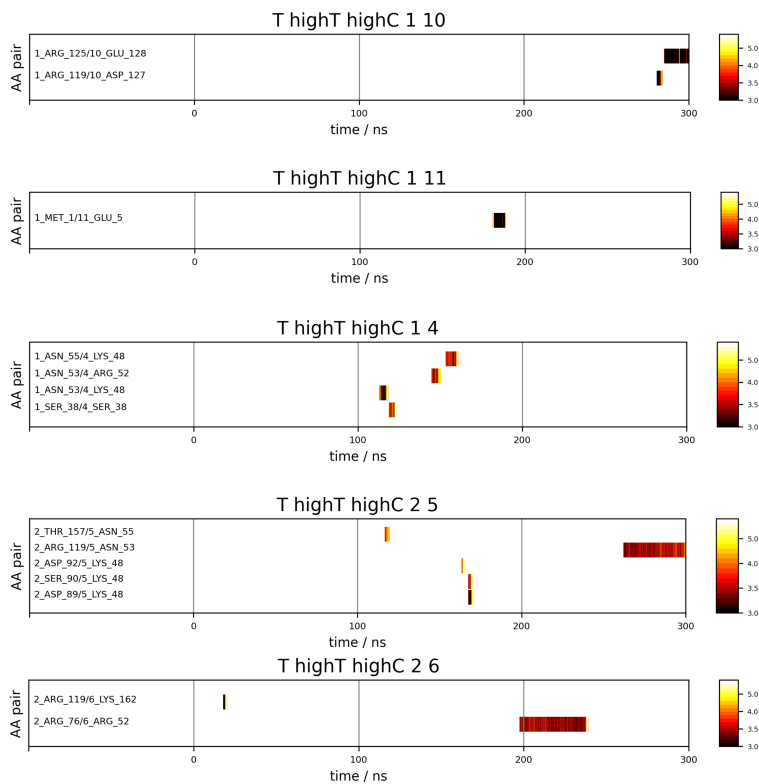


Figure S20: Time evolution of residue-residue contacts that appear within  $6 \text{ \AA}$  between different pairs of T4 WT\* molecules in the solution comprising of  $90 \text{ mg mL}^{-1}$  of T4 WT\* at 300 K. The shortest distance (here in  $\text{\AA}$ ) between the residue pairs is represented with a heat map on the right. Distances above  $6 \text{ \AA}$  are plotted as white space.

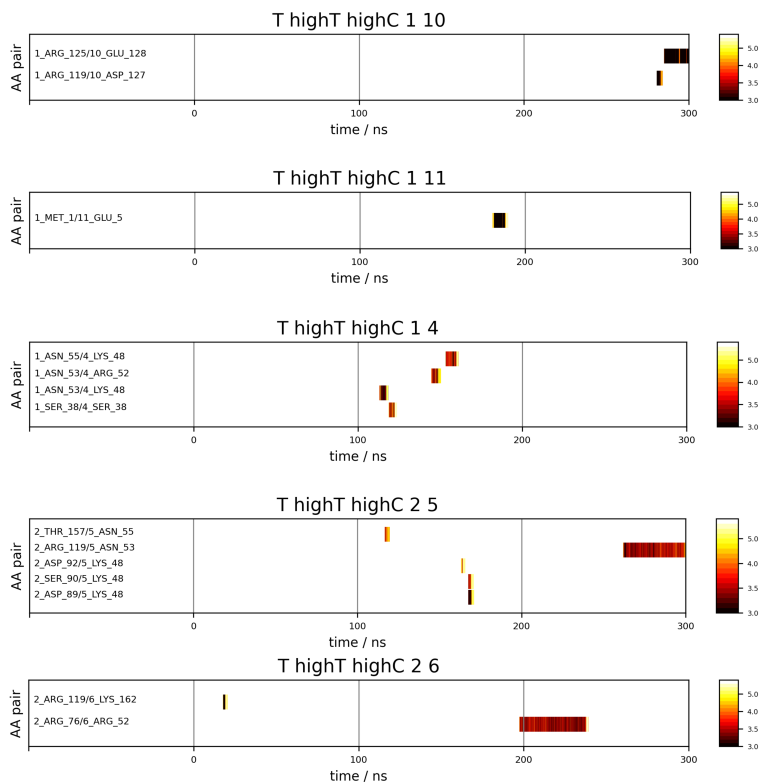


Figure S21: Time evolution of residue-residue contacts that appear within  $6 \text{ \AA}$  between different pairs of T4 WT\* molecules in the solution comprising of  $90 \text{ mg mL}^{-1}$  of T4 WT\* at 300 K. The shortest distance (here in  $\text{\AA}$ ) between the residue pairs is represented with a heat map on the right. Distances above  $6 \text{ \AA}$  are plotted as white space.

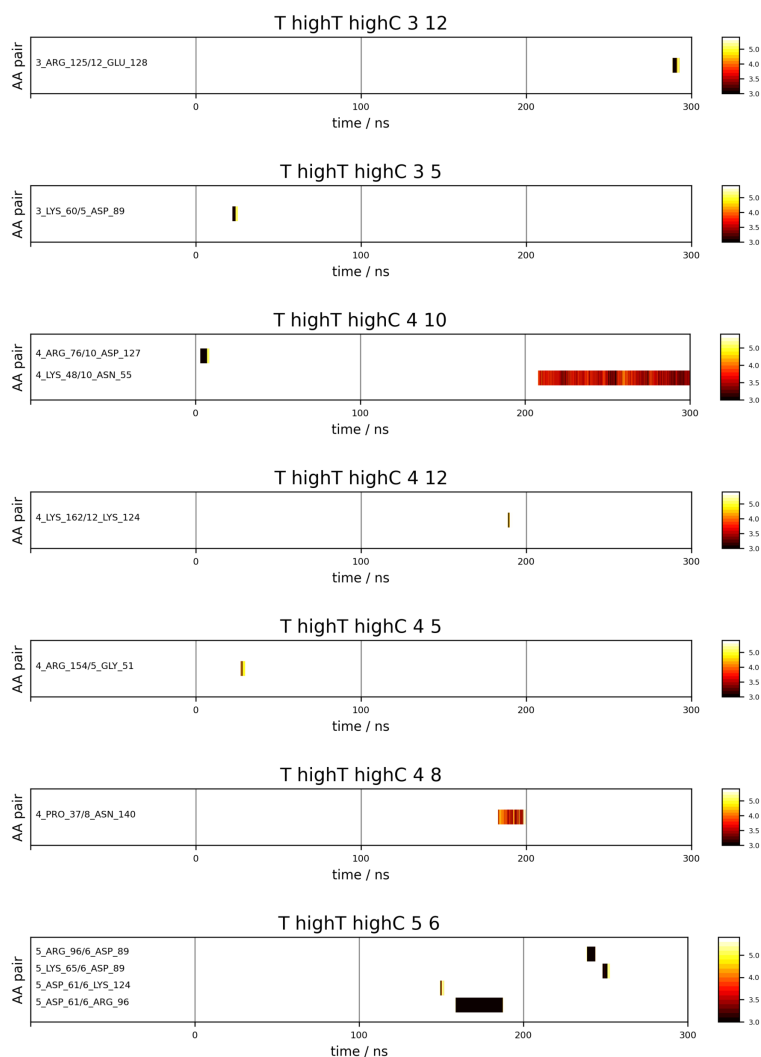


Figure S22: Time evolution of residue-residue contacts that appear within 6 Å between different pairs of T4 WT\* molecules in the solution comprising of 90 mg mL<sup>-1</sup> of T4 WT\* at 300 K. The shortest distance (here in Å) between the residue pairs is represented with a heat map on the right. Distances above 6 Å are plotted as white space.

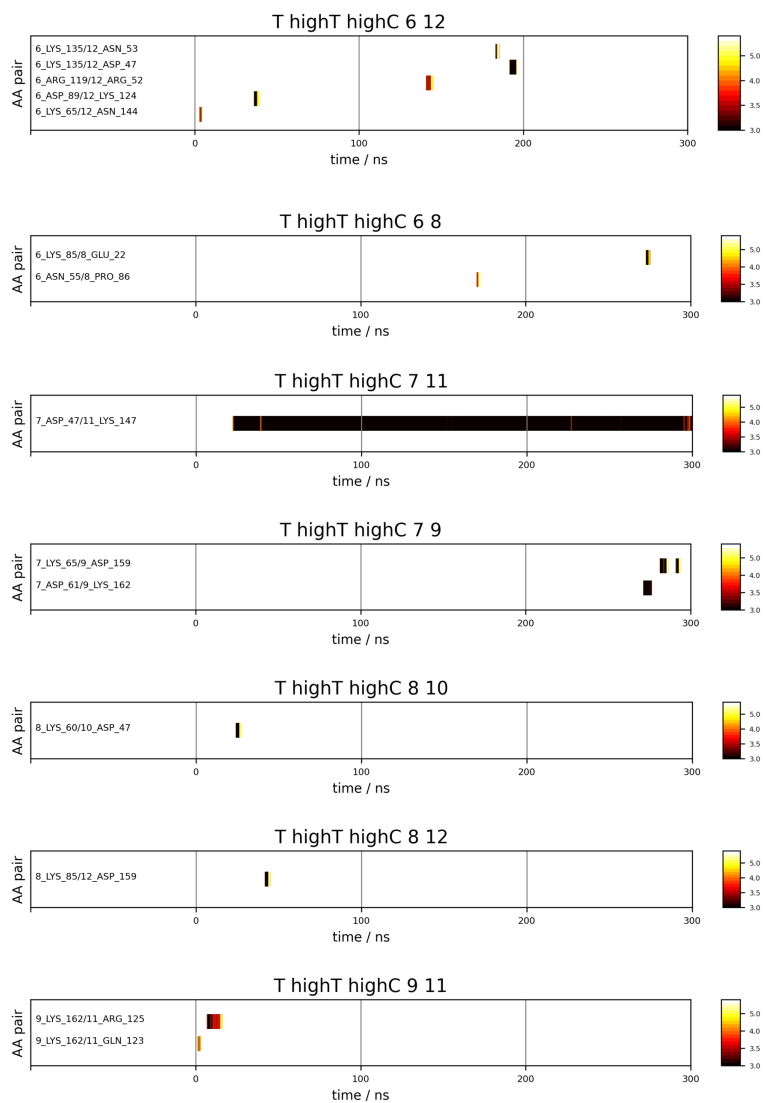


Figure S23: Time evolution of residue-residue contacts that appear within 6 Å between different pairs of T4 WT\* molecules in the solution comprising of 90 mg mL<sup>-1</sup> of T4 WT\* at 300 K. The shortest distance (here in Å) between the residue pairs is represented with a heat map on the right. Distances above 6 Å are plotted as white space.

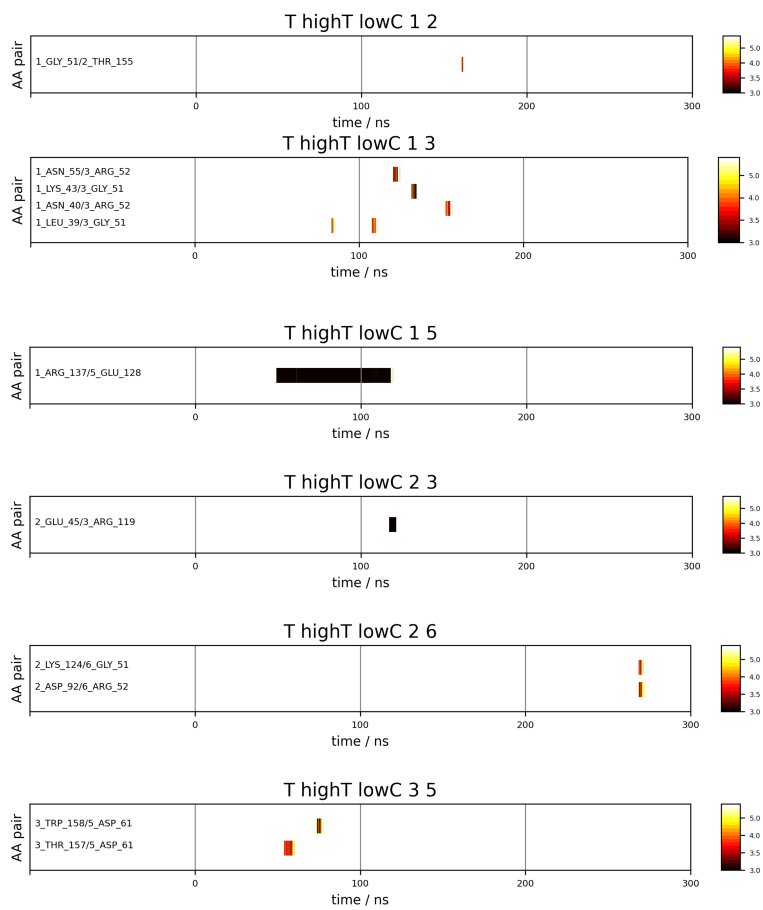


Figure S24: Time evolution of residue-residue contacts that appear within  $6 \text{ \AA}$  between different pairs of T4 WT\* molecules in the solution comprising of  $45 \text{ mg mL}^{-1}$  of T4 WT\* at 300 K. The shortest distance (here in  $\text{\AA}$ ) between the residue pairs is represented with a heat map on the right. Distances above  $6 \text{ \AA}$  are plotted as white space.

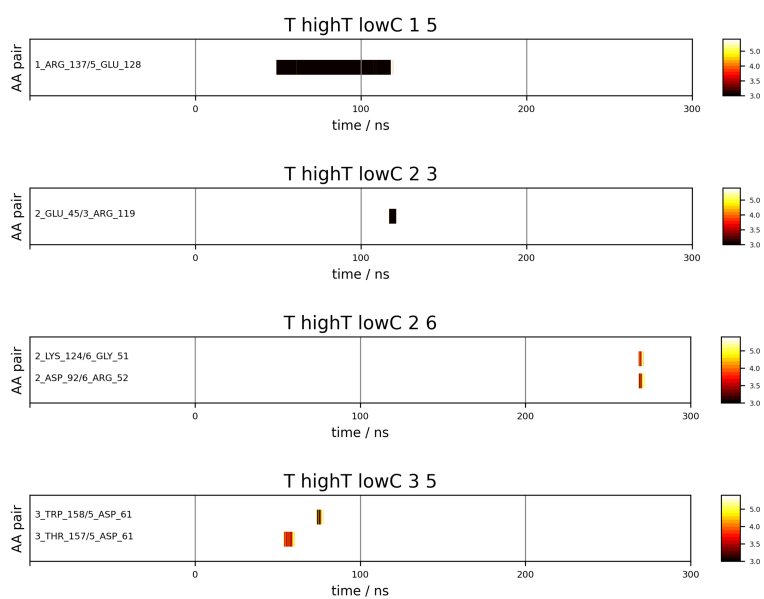


Figure S25: Time evolution of residue-residue contacts that appear within  $6 \text{ \AA}$  between different pairs of T4 WT\* molecules in the solution comprising of  $45 \text{ mg mL}^{-1}$  of T4 WT\* at 300 K. The shortest distance (here in  $\text{\AA}$ ) between the residue pairs is represented with a heat map on the right. Distances above  $6 \text{ \AA}$  are plotted as white space.

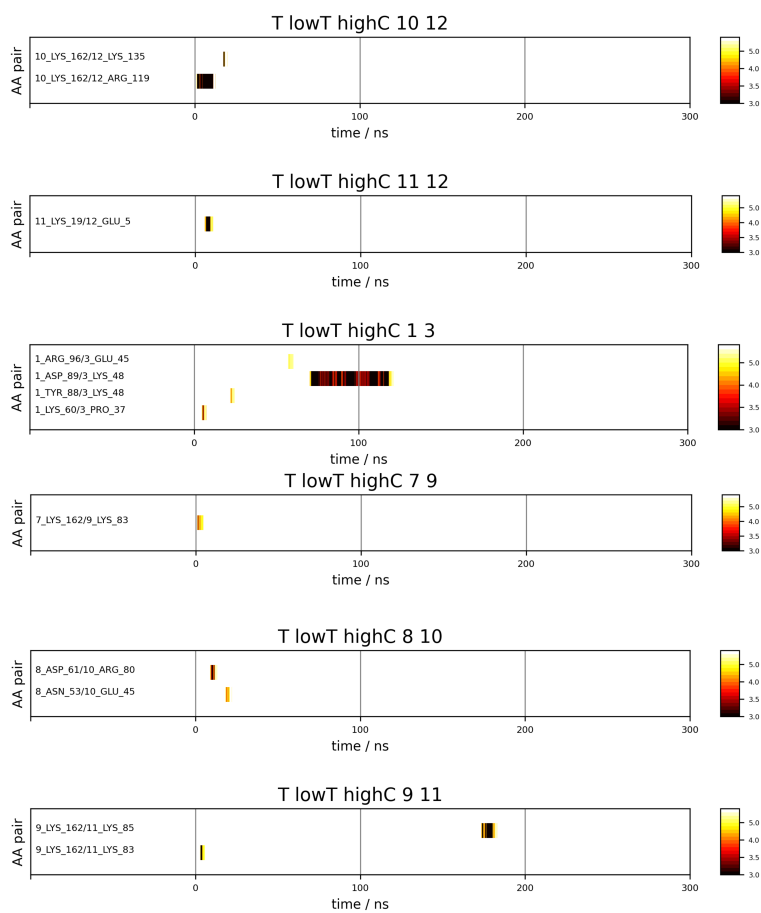


Figure S26: Time evolution of residue-residue contacts that appear within  $6 \text{ \AA}$  between different pairs of T4 WT\* molecules in the solution comprising of  $90 \text{ mg mL}^{-1}$  of T4 WT\* at 267 K. The shortest distance (here in  $\text{\AA}$ ) between the residue pairs is represented with a heat map on the right. Distances above  $6 \text{ \AA}$  are plotted as white space.

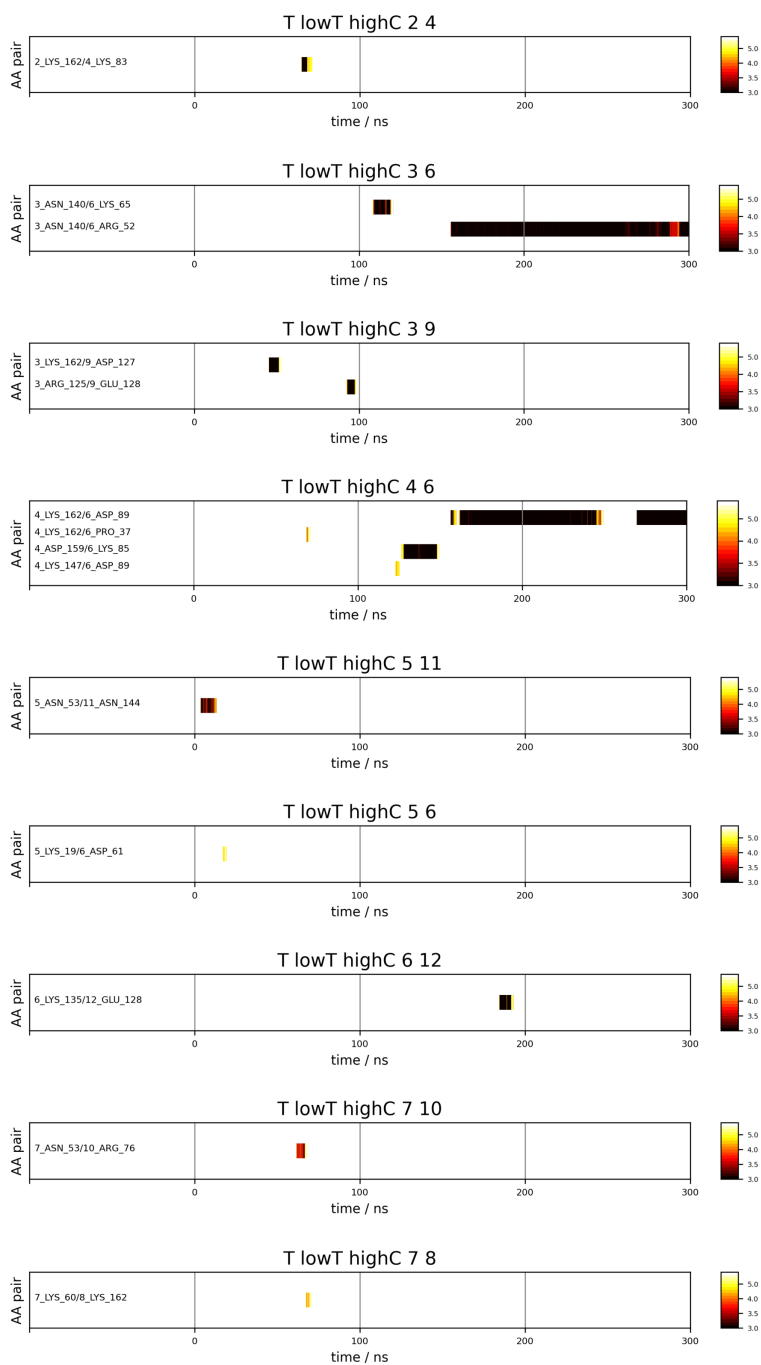


Figure S27: Time evolution of residue-residue contacts that appear within 6 Å between different pairs of T4 WT\* molecules in the solution comprising of 90 mg mL<sup>-1</sup> of T4 WT\* at 267 K. The shortest distance (here in Å) between the residue pairs is represented with a heat map on the right. Distances above 6 Å are plotted as white space.

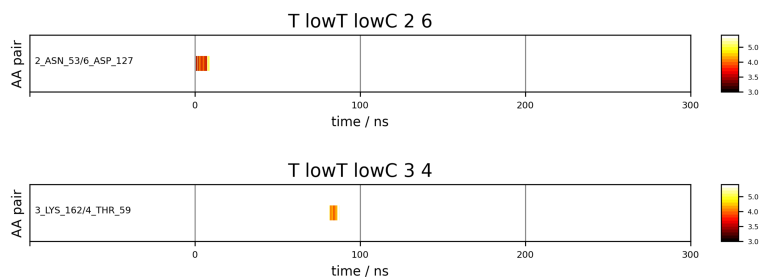


Figure S28: Time evolution of residue-residue contacts that appear within  $6 \text{ \AA}$  between different pairs of T4 WT\* molecules in the solution comprising of  $45 \text{ mg mL}^{-1}$  of T4 WT\* at 267 K. The shortest distance (here in  $\text{\AA}$ ) between the residue pairs is represented with a heat map on the right. Distances above  $6 \text{ \AA}$  are plotted as white space.

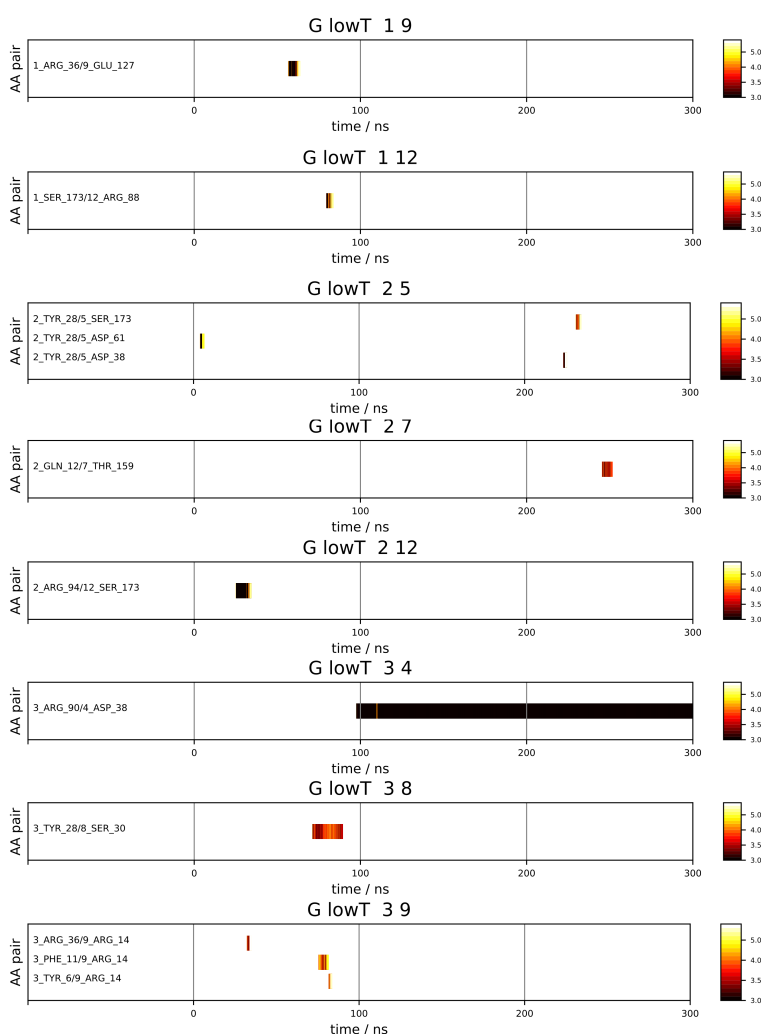


Figure S29: Time evolution of residue-residue contacts that appear within  $6 \text{ \AA}$  between different pairs of  $\gamma$ -D crystallin molecules in the solution comprising of  $100 \text{ mg mL}^{-1}$  of  $\gamma$ -D crystallin at 300 K. The shortest distance (here in  $\text{\AA}$ ) between the residue pairs is represented with a heat map on the right. Distances above  $6 \text{ \AA}$  are plotted as white space.

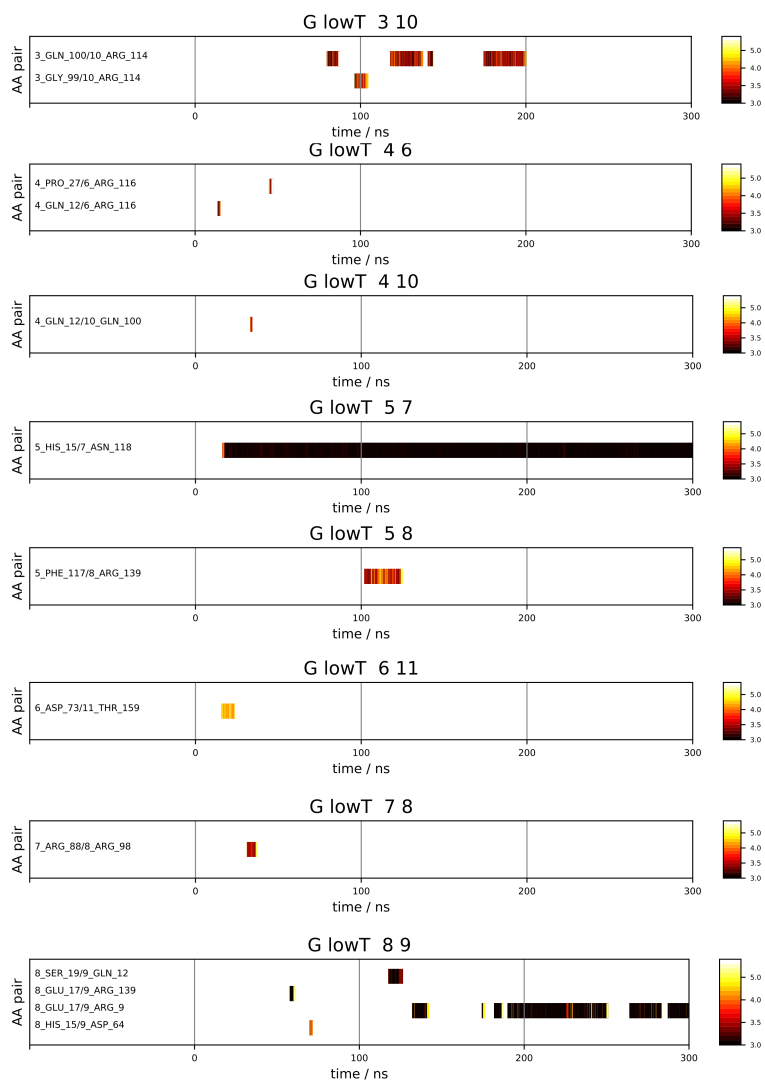


Figure S30: Time evolution of residue-residue contacts that appear within 6 Å between different pairs of  $\gamma$ -D crystallin molecules in the solution comprising of 100 mg mL<sup>-1</sup> of  $\gamma$ -D crystallin at 300 K. The shortest distance (here in Å) between the residue pairs is represented with a heat map on the right. Distances above 6 Å are plotted as white space.

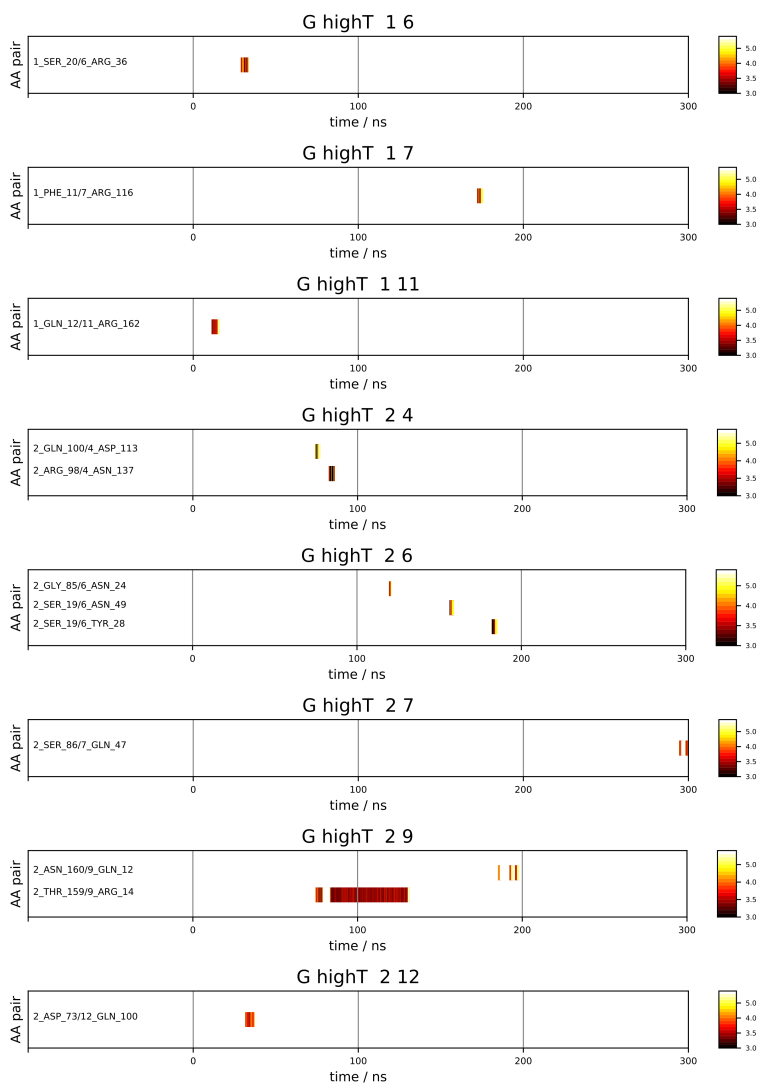


Figure S31: Time evolution of residue-residue contacts that appear within 6 Å between different pairs of  $\gamma$ -D crystallin molecules in the solution comprising of 100 mg mL<sup>-1</sup> of  $\gamma$ -D crystallin at 320 K. The shortest distance (here in Å) between the residue pairs is represented with a heat map on the right. Distances above 6 Å are plotted as white space.

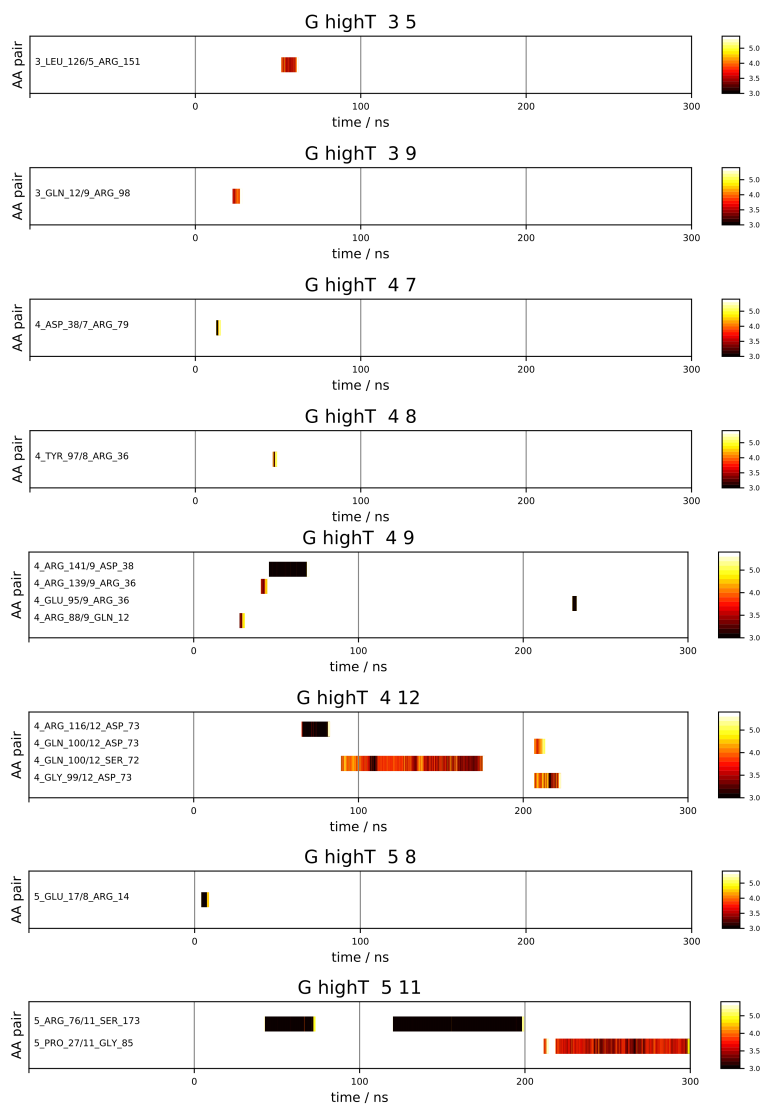


Figure S32: Time evolution of residue-residue contacts that appear within 6 Å between different pairs of  $\gamma$ -D crystallin molecules in the solution comprising of 100 mg mL<sup>-1</sup> of  $\gamma$ -D crystallin at 320 K. The shortest distance (here in Å) between the residue pairs is represented with a heat map on the right. Distances above 6 Å are plotted as white space.

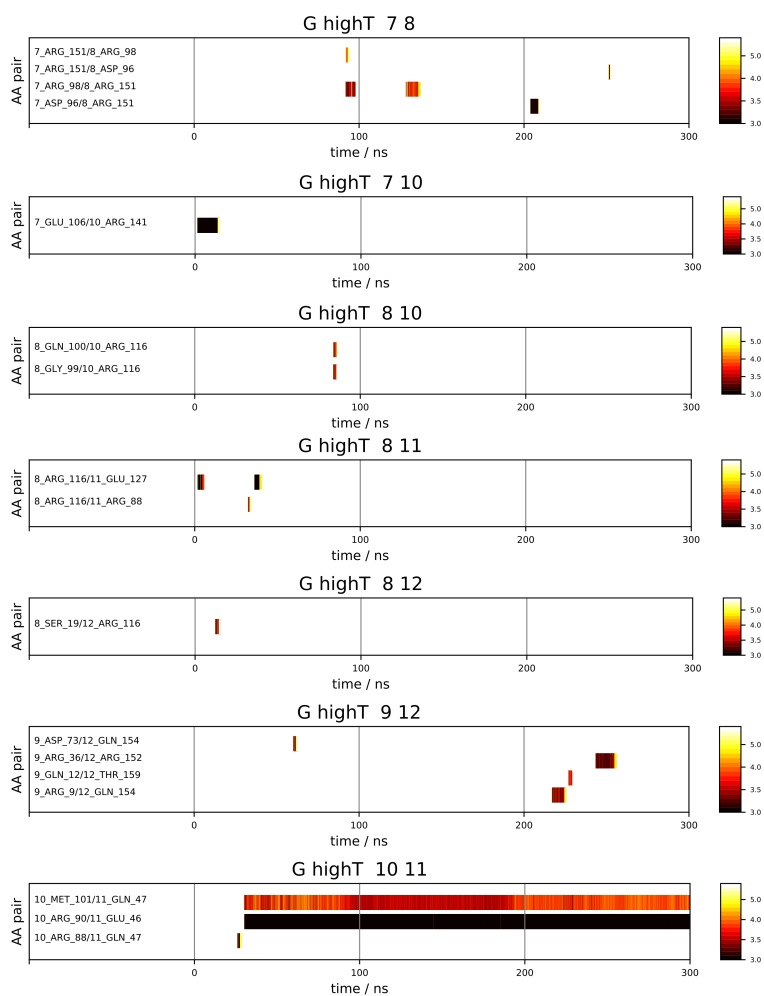


Figure S33: Time evolution of residue-residue contacts that appear within 6 Å between different pairs of  $\gamma$ -D crystallin molecules in the solution comprising of 100 mg mL<sup>-1</sup> of  $\gamma$ -D crystallin at 320 K. The shortest distance (here in Å) between the residue pairs is represented with a heat map on the right. Distances above 6 Å are plotted as white space.